



## Research article

# Salinity levels influence treatment performance and the activity of electroactive microorganisms in a microbial fuel cell system for wastewater treatment

Antonio Castellano-Hinojosa <sup>a,b,\*</sup> , Manuel J. Gallardo-Altamirano <sup>a</sup> , Clementina Pozo <sup>a,b</sup>,  
Alejandro González-Martínez <sup>a,b</sup>, Jesús González-López <sup>a,b</sup>, Ian P.G. Marshall <sup>c</sup> 

<sup>a</sup> Environmental Microbiology Group, Institute of Water Research, University of Granada, 18003, Granada, Spain

<sup>b</sup> Department of Microbiology, University of Granada, 18071, Granada, Spain

<sup>c</sup> Center for Electromicrobiology, Department of Biology, Aarhus University, Aarhus, Denmark



## ARTICLE INFO

## Keywords:

Wastewater  
Anode biofilm  
Electroactive microorganisms  
Current production  
Metagenomics  
Metatranscriptomics

## ABSTRACT

There is growing interest in developing effective treatment technologies to mitigate the environmental impact of saline wastewater while also potentially recovering valuable resources from it. However, it remains largely unknown how different salinity levels impact treatment performance, energy generation, and the diversity and composition of electroactive microorganisms in MFCs treating real effluents such as urban wastewater. This study explores the impact of three salinity levels (3.5, 7, and 15 g/L NaCl) on current production, organic removal rates, and bacterial community dynamics in a continuous-flow microbial fuel cell (MFC) fed with urban wastewater. Using metagenomics and metatranscriptomics, we explored variations in the abundance and expression of extracellular electron transfer (EET) genes and those involved in other general metabolisms. We found that low salinity (3.5 g/L NaCl) enhanced both current production and organic removal efficiency compared to higher salinity levels. This improvement was linked to an increased abundance and activity of electroactive microorganisms, particularly taxa within the Ignavibacteria class, which possess genes coding for outer membrane cytochromes and porin cytochromes. Additionally, salinity influenced general metabolic genes and microbial community composition, with higher salinity levels limiting bacterial growth and diversity. This research provides valuable insights into the interplay between salinity stress and microbial adaptation, contributing to the optimization of MFC technologies for enhanced environmental and bioengineering applications.

## 1. Introduction

Industrial processes such as seafood processing, oil and gas production, mining, desalination, and the use of seawater for different activities (e.g., flushing toilets, cleaning, and defrosting) produce saline wastewater (He et al., 2017). In addition, urban wastewater treatment plants (WWTPs) located in coastal regions are often exposed to seawater infiltration resulting in saline wastewater (Egea-Corbacho et al., 2021). The effective treatment of saline wastewater is a major environmental and economic challenge, as high salinity can severely inhibit microbial activity in biological treatment systems while also increasing the energy demand and operational costs of conventional treatment technologies.

This issue is particularly critical in water-scarce regions, where the reuse of treated wastewater is necessary to alleviate freshwater shortages. Developing cost-effective, energy-efficient, and environmentally sustainable solutions for saline wastewater treatment is therefore an urgent global priority (Tan et al., 2019).

Conventional physical and chemical technologies such as physical adsorption, membrane separation, ion exchange, and advanced oxidation processes, have long been used to treat saline wastewater (Alam et al., 2022). However, these methods are plagued by significant drawbacks including high operational costs, generation of secondary pollutants, and lack of bioresource/bioenergy recovery (Velasco et al., 2019; Tan et al., 2019). From an economic perspective, the high capital

\* Corresponding author. Environmental Microbiology Group, Institute of Water Research, University of Granada, 18003, Granada, Spain, Department of Microbiology, University of Granada, 18071, Granada, Spain.

E-mail address: [ach@ugr.es](mailto:ach@ugr.es) (A. Castellano-Hinojosa).

<https://doi.org/10.1016/j.jenvman.2025.124858>

Received 15 November 2024; Received in revised form 11 February 2025; Accepted 4 March 2025

Available online 9 March 2025

0301-4797/© 2025 Elsevier Ltd. All rights reserved, including those for text and data mining, AI training, and similar technologies.

and maintenance costs of these conventional treatments often limit their implementation in low- and middle-income countries, where access to cost-effective wastewater treatment technologies is essential for public health and environmental protection (Velasco et al., 2019; Tan et al., 2019). Additionally, the growing regulatory pressure on industries to manage their saline effluents more sustainably highlights the need for innovative and scalable solutions. Consequently, there is a growing need for cost-effective and sustainable treatment alternatives that not only remove pollutants from saline wastewater but also facilitate resource recovery. Biological approaches have emerged as an alternative approach for saline wastewater treatment, leveraging the metabolic capabilities of microorganisms to degrade organic pollutants. Various bioreactor configurations, such as sequencing batch reactors (SBR), biofilm sequencing batch reactors (BSBR), upflow anaerobic sludge blanket (UASB) reactors, and other anaerobic-aerobic processes, have been successfully employed in this regard (He et al., 2017; Alam et al., 2022). However, these systems face significant challenges, primarily due to the limited ability of most microbial communities to tolerate high salinity, which can disrupt metabolic activity and reduce treatment efficiency. Consequently, a better understanding of microbial adaptation to saline conditions is essential to optimize biological treatment approaches.

Bioelectrochemical systems such as microbial fuel cells (MFCs) have received increased interest as a promising and sustainable approach for treating urban and industrial wastewater while producing electricity (Kim et al., 2013; Guo et al., 2021; Tsekouras et al., 2022). MFCs harness the metabolic activity of microorganisms to oxidize organic matter in wastewater, producing electrons that flow through an external circuit, generating electrical energy (Logan et al., 2006). From an economic perspective, the integration of MFCs into wastewater treatment plants could reduce energy costs, provide decentralized energy sources, and improve the financial viability of wastewater treatment operations (Guo et al., 2021). Previous research has demonstrated the potential of saline wastewater to support power generation in MFCs owing to its greater ionic conductivity (~7–20 mS/cm) compared to regular wastewater (~1 mS/cm) (Lefebvre et al., 2006, 2012; Li et al., 2013; Guo et al., 2021; Saravanan et al., 2023). However, most of these studies were run in MFCs under fed-batch mode for limited periods of time (e.g., 6–24 h) and were fed with synthetic medium simulating real wastewater, limiting their applicability to real wastewater treatment scenarios. Continuous-flow MFCs are more suitable for practical applications compared to batch-mode MFCs as they can treat larger volumes for longer periods of time (Chung et al., 2009; Cai et al., 2014; Cabrera et al., 2022). In addition, real effluents contain more complex carbon sources than synthetic media which may determine variations in anode colonization, microbial community composition, and subsequent current production. Therefore, additional research is needed on the use of continuous-flow MFCs to treat real wastewater under different salinity levels to fully understand the impact of salinity on organic matter removal, current production, and the anode microbiome.

A key drawback in the biological treatment of saline wastewater persists due to the limited ability of microorganisms to adapt to high salinity levels (Lefebvre et al., 2006; 2012). The high salt content of saline wastewater can create challenges for microbial activity and electrode performance in MFCs. Still, certain exoelectrogens (microorganisms that transfer electrons to a solid electrode) can thrive in these conditions, enhancing the efficiency of MFCs (Guo et al., 2021). However, increasing the ionic strength will not always improve electricity generation (Miyahara et al., 2015; Guo et al., 2021; Pang et al., 2024). When the electrolyte salinity exceeds the threshold that exoelectrogens can deal with, the current production ability of the bacteria is inhibited (Li et al., 2013; Guo et al., 2021; Xin et al., 2022). Previous studies have found that exoelectrogens such as *Geobacter*, *Pseudomonas*, *Bacillus*, *Desulfuromonas*, and *Aeromonas* species can tolerate saline conditions up to ~ 55 mS/cm (Sun et al., 2014; Miyahara et al., 2015; Guo et al., 2021). Yet, it remains largely unknown how different salinity levels

impact the diversity and composition of electroactive microorganisms in MFCs treating real effluents such as wastewater. This information can help not only understand how exoelectrogens may adapt and evolve with time but to select optimal salinity levels for enhancing current generation in these bioelectrochemical systems.

Exoelectrogenic microorganisms play a pivotal role in MFCs generating electrical currents through the oxidation of OM and transferring electrons to the anode (Kock and Harnish, 2016; Logan et al., 2019; Castellano-Hinojosa et al., 2022). Metagenomic and metatranscriptomic analyses are being increasingly used to understand the genetic potential, functional activity, and functional adaptability of exoelectrogens in MFCs. For example, these tools can help characterize variations in the abundance and expression of extra-cellular electron transfer (EET) genes under contrasting conditions and help identify key electroactive taxa (Ishii et al., 2013; Mickol et al., 2021; Cai et al., 2022; Wu et al., 2022; Olmsted et al., 2023; Lustermans et al., 2024). Given the potential impact of salinity on microbial metabolism, investigating the expression of EET genes under different salinity conditions could provide valuable insights for improving MFC efficiency. Several pathways for EET (e.g., porin-cytochrome complexes) have been identified in model electroactive organisms, including *Geobacter sulfurreducens*, *Shewanella oneidensis*, and *Pseudomonas putida* (Logan et al., 2019; Lovley and Holmes, 2021; Paquete et al., 2022). EET is widespread, suggesting that other microorganisms may possess different pathways for EET (Shi et al., 2016; Zhong and Shi, 2018; Baker et al., 2022). In Gram-negative bacteria, the presence of an outer membrane necessitates specific adaptations for EET, such as outer membrane cytochromes or porin-cytochrome complexes that can shuttle electrons across this barrier (Wrighton et al., 2011; Lovley and Holmes, 2021; Paquete et al., 2022). The thick peptidoglycan layer of Gram-positive bacteria poses a different challenge for electron transfer, typically requiring unique mechanisms to bridge the distance to the external environment (Wrighton et al., 2011; Lovley and Holmes, 2021; Paquete et al., 2022). While salinity gradients are known to shape EET gene abundance in estuarine and marine sediments (Fortunato et al., 2015; Ji et al., 2022), little is known about their effects on wastewater-fed MFCs. Moreover, the impact of salinity on broader microbial metabolisms (e.g., carbon fixation, methane, and nitrogen cycles) in MFCs remains largely unexplored, yet it could be crucial for optimizing treatment performance.

The objective of this study was to examine the impact of three different salinity levels on current production, treatment performance, and the abundance and expression of EET genes in a continuous-flow MFC fed with urban wastewater. Variations in the abundance and activity of exoelectrogenic microorganisms were studied and their relative importance for explaining variations in current production under different salinity levels was explored. Impacts of salinity levels on the presence and expression of genes involved in other general metabolisms were also studied. The effect of salinity on the abundance, diversity, and composition of bacterial communities was also examined to get additional insights into the anode microbiome.

## 2. Materials and methods

### 2.1. Design and operation of the MFC system

A two-chambered H-cell type MFC was used in this study (Fig. S1). The MFC consisted of two cylindrical chambers of methacrylate with a volume of 5 L for the anode (height of 60 cm and diameter of 10 cm) and 4 L for the cathode (height of 50 cm and diameter of 10 cm). The chambers were separated by a proton exchange membrane (Nafion N117, Chemours, Italy) which was pre-treated as recommended by the manufacturer. The anode was made of carbon fibers (PANEX 35 50K, Zoltek, Mill-Rose, OH, USA; 6.35 mm thickness; 240 cm<sup>2</sup> projected area) and the cathode consisted of a copper bar (17 cm<sup>2</sup> projected area). Both chambers were connected using a copper conductor cable for electron transport. Sensors for measurements of redox potential, pH,

temperature, and dissolved oxygen concentrations were placed in both chambers. The MFC was operated in continuous-flow mode.

In separate experiments, the anode chamber was inoculated with 4 L of activated sludge taken from the aeration tank of the municipal WWTP “EDAR SUR” (EMASAGRA S.A., Granada, Spain). The biomass concentration in the activated sludge was quantified by measuring the mixed liquor suspended solids (MLSS) and varied between 2.9 and 3.1 g/L. Before starting the experiments, the inoculum was recirculated for 4 days at  $4 \text{ L h}^{-1}$  and continuously mixed using a magnetic stirrer at 1500 rpm to favor anode colonization. The anode chamber was fed using a peristaltic pump with wastewater collected every three days from the primary settling tank of the WWTP as mentioned earlier. A hydraulic retention time of 1 day was used in this study to maximize electricity generation based on previous experiments (Castellano-Hinojosa et al., 2024, 2025). In separate experiments, the influent wastewater was amended with NaCl at three different salinity levels: low (3.5 g/L, LW treatment), medium (7.0 g/L, ME treatment), and high (15 g/L, HG treatment). Unamended wastewater was used as a control (CT treatment). Each of the treatments was assayed for 30 days. The total duration of the experiment was 4 months. The different salinity levels were selected to cover a broad range of salt concentrations commonly reported in urban and industrial wastewater (Cortés-Lorenzo et al., 2015; Correa-Galeote et al., 2021). The MFC was cleaned between experiments and the carbon fibers of the anode were replaced. The catholyte was fed with a phosphate buffer (Rossi and Logan, 2020) which was renewed every week. The catholyte was continuously sparged with air ( $9 \text{ mg L}^{-1}$ ). The anode and cathode chambers were continuously mixed using a magnetic stirrer at 1500 rpm. The MFC was operated at 20–22 °C in a controlled-temperature room.

## 2.2. Electrochemical and physiochemical measurements

To monitor the changes in voltage production (mV) during the experimental period, a Supervisory Control and Data Acquisition (SCADA) software together with a Programmable Logic Controller (PLC) were used. The data were read by the PLC and automatically saved in the internal memory. The MFC was operated using an external resistance of 100  $\Omega$  to maximize electricity generation (Castellano-Hinojosa et al., 2024). Current production was calculated applying Ohm's law ( $I = V/R$ ), where  $V$  is the measured voltage (volt), and  $R$  is the external resistance (ohm). The current density ( $j$ ;  $\text{mA m}^{-2}$ ) in the anode was calculated according to the projected anode surface area using the equation ( $j = V/R_{\text{ext}} \times A_{\text{An}}$ ) where  $V$  is the voltage (volt),  $R_{\text{ext}}$  is the external resistance (ohm), and  $A_{\text{An}}$  is the projected anode area in  $\text{m}^2$  (Logan et al., 2008). The coulombic efficiency (CE) was calculated as described by Logan et al. (2008).

Water samples from the influent and effluent were collected twice per week and used for physicochemical analyses. The chemical oxygen demand (COD) and concentration of suspended solids were determined using standard methods (APHA, 2012). The organic loading rate in the influent ( $\text{mg COD L}^{-1} \text{ d}^{-1}$ ) and organic removal rate (differences in COD content between the effluent and influent) were calculated. Biomass concentration in the inoculum was determined by measuring the mixed liquor suspended solids (MLSS) (APHA, 2012). The concentrations of ammonium ( $\text{NH}_4^+$ ) and nitrate ( $\text{NO}_3^-$ ) were measured by ion chromatography as described by Castellano-Hinojosa et al. (2024) and the N removal % was calculated based on differences in  $\text{NH}_4^+ + \text{NO}_3^-$  concentrations between the effluent and influent. Variations in pH were continuously monitored using sensors placed in the anode chamber. Conductivity was measured with a laboratory conductivity meter sensor + pH 3 (Hach Lange, Ames, USA).

## 2.3. Biomass collection and DNA and RNA extraction

Biomass from the anode was collected after 0 (original inoculum), 10, 20, and 30 days of operation for each treatment. Water samples from

the influent wastewater (prior to any salt addition) were also collected in parallel during the experimental period. The anode biofilm was scraped from the anode using pre-sterilized tweezers and suspended in 30 mL of sterilized saline solution (0.9% NaCl). Anode biofilm and water samples were centrifuged at 13,000 rpm for 5 min and the pelleted biomass was kept at  $-80 \text{ }^\circ\text{C}$  until use. The FastDNA SPIN Kit and the FastRNA™ Pro Soil-Direct Kit (MP Biomedicals, Solon, OH, USA) were used for DNA and RNA extractions, respectively. The concentration of DNA and RNA was determined using the Qubit™ dsDNA High Sensitivity assay and Qubit™ RNA High Sensitivity assay kits (Thermo Fisher Scientific, USA), respectively.

## 2.4. qPCR analysis

The absolute abundance of bacteria was determined by qPCR using the primer pairs 341F (5'-CCTAYGGGRBGCASCAG-3') and 806R (5'-GGACTACHVGGGTWTCAAT-3') (Yu et al., 2005). The qPCR was performed using a QuantStudio 3 Real-Time PCR system (ThermoFisher, USA) and PCR mixtures and conditions described earlier [45]. The calibration curves showed a good correlation coefficient ( $R^2 = 0.999$ ). The quality of qPCR amplification was also verified by melting curve analysis and electrophoresis in agarose.

## 2.5. 16S rRNA amplicon community analysis

The V3-V4 region of the bacterial 16S rRNA gene was amplified using the primer pairs 341F/806R. Samples were sequenced in an Illumina MiSeq sequencer by Novogene Europe (Cambridge, UK). The sequence reads were processed in QIIME2 following the methods described in full detail by Castellano-Hinojosa et al. (2023). Briefly, the sequences were assembled and dereplicated into representative amplicon sequence variants (ASVs) using dada2 v.1.26.0 (Callahan et al., 2016), and then classified using the SILVA database version 138 (Quast et al., 2013) using the naïve Bayes classifier in QIIME2 (Bolyen et al., 2019). The final dataset consisted of a mean of 62,189 sequences per sample. Alpha and beta diversity analyses were done using the packages “vegan” v.2.5–2 (Oksanen et al., 2024) and “Phyloseq” v.1.24.0 (McMurdie and Holmes, 2013) in the R software. Changes in the composition of the bacterial community between time points were evaluated by permutational analysis of variance (PERMANOVA) in R. Differentially abundant bacterial genera between the LW, ME, and HG treatments compared to CT were detected after 30 days of operation using the DESeq2 analysis (Love et al., 2014).

## 2.6. Metagenomics

Metagenome sequencing (2x 150 bp, 15 GB reads/sample) was done with Illumina HiSeq (Illumina, USA) by Novogene Europe (Cambridge, UK). Reads were quality-checked using FastQC v.0.12.0 (Andrews, 2014) and sequences were trimmed and size-filtered using Trimmomatic v.0.39 with settings HEADCROP:5, SLIDINGWINDOW:4:20 and MINLEN:100 (Bolger et al., 2014). Overall community composition at the kingdom, phylum, and genus taxonomic levels of the raw metagenomics data was conducted using phyloflash v.3.4.2 (Gruber-Vodicka et al., 2020). The metagenomes from all samples were *de novo* assembled using MEGAHIT v.1.2.9 (Li et al., 2015). Protein-coding genes were predicted using Prodigal v2.6.3 (Hyatt et al., 2010). Reads from sequencing libraries were mapped using BMap v39.06 (Bushnell, 2014) and converted to the bam file format using SAMtools version 1.20 (Li et al., 2009). The metagenomes were binned using MetaBat2 version 2.15.2 with the parameter `-superspecific` (Kang et al., 2019) to form metagenome-assembled genomes (MAGs). The quality of the genome assembly and the completeness and contamination of the genome bins were assessed using Quast v.5.2.0 (Mikheenko et al., 2018) and CheckM2 version 1.0.2 (Chklovski et al., 2023), respectively. Bins were taxonomically classified with GTDB-tk v2.1.1 and database r220

(Chaumeil et al., 2022). The final collection of protein-coding genes and bins were functionally characterized through KOfams v1.3.0 (Aramaki et al., 2020) with default cut-off values for selected KOs and through the FeGenie database v.1.2. for genes involved in iron metabolism (Garber et al., 2020). The taxonomic composition of taxa containing EET genes was examined using Blastp (Camacho et al., 2009) against the nr database. Genes coding for  $\text{Na}^+/\text{H}^+$  antiporters (e.g., *nhaA*, *nhaB*, *nhaC*, *nhaP*, *mnhA*, and *mrpA*) in the MAGs involved in EET were identified and annotated using PROKKA (Seemann et al., 2014). A phylogenetic tree for all EET MAGs was generated by making a concatenated multiple sequence alignment of core proteins using the identify and align workflows from GTDB-tk v.2.3.0 (Chaumeil et al., 2022) and then producing a phylogenetic tree using IQ-TREE version 2.3.5 (Minh et al., 2020) with “-m TEST” to automatically determine the best model and “-b 100” to find the consensus tree from 100 bootstraps.

## 2.7. Metatranscriptomics

Metatranscriptome sequencing was done (2x 150 bp, 15 GB reads/sample) with Illumina HiSeq (Illumina, USA) with rRNA removal by Novogene Europe (Cambridge, UK). Reads were quality-checked using FastQC v.0.12.0 (Andrews, 2010) and sequences were trimmed and size-filtered using Trimmomatic v.0.39 (Bolger et al., 2014). Trimmed sequences were mapped against the metagenomic assembly with BMap v39.06 to determine transcript abundance (Bushnell, 2014). Protein-coding genes were identified in assembled transcripts using Prodigal v2.6.3 (Hyatt et al., 2010).

## 2.8. Genome and statistical analyses

A summary of raw sequencing information for the metagenomic and metatranscriptomic samples is provided in Table S1. To explore the

impact of salinity on different metabolic pathways, we selected KOs associated to eleven different cycles including carbon fixation, central metabolism, methane metabolism, fermentation, nitrogen metabolism, sulfur metabolism, oxidative phosphorylation, secretion system, phosphorus metabolism, iron metabolism, and other metabolisms from the KEGG database (<https://www.kegg.jp>) (Table S2). For each selected cycle, principal coordinates analyses (PCoA) based on the Bray–Curtis distance were done to explore variations in the functional and taxonomical profiles of the metagenomes and metatranscriptomes over time. The taxonomic and functional profiles were obtained by grouping the samples by contig IDs or KOs, respectively. Analysis of similarities (ANOSIM) was used to evaluate the significance of differences between treatments. PCoA and ANOSIM analyses were done using the vegan package v.2.6–6.1 in R.

Differences in electrochemical (current production and current density), physicochemical (organic loading rate, organic removal rate, N removal %, conductivity, pH,  $\text{NH}_4^+$ ,  $\text{NO}_3^-$ ), and microbial (qPCR and alpha diversity indices) parameters were analyzed using linear mixed-effects (LME) models with treatment, time point, and their interactions considered as random factors using the “lme4” package v.1.1–35.5 in R (Bates et al., 2015). Significant effects were determined by analysis of variance (ANOVA) ( $p \leq 0.05$ ). LME models were also used to study the contribution of active MAGs containing EET genes as controllers of changes in current production. All the statistical analyses were performed and visualized using the R software version 4.0.5 (<http://www.rproject.org/>).

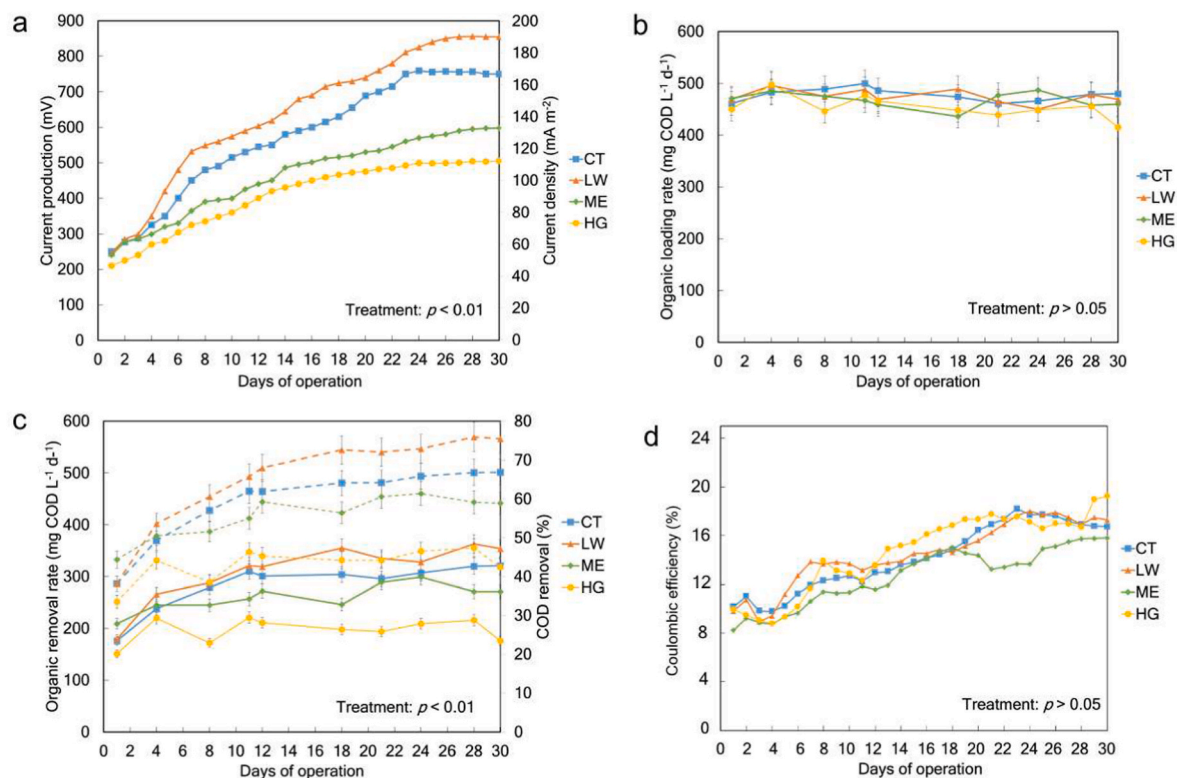


**Fig. 1.** Variations in current production and current density (a), organic loading rate (b), organic removal rate (solid line) and COD removal % (dotted line) (c), and coulombic efficiency (d) during the experimental period for the different treatments. Treatments are named as follows: CT, control; LW, low salinity; ME, medium salinity; HG, high salinity. Values are expressed as mean with standard error. Linear mixed-effects models were used to look for significant differences between treatments. Significant effects were determined by ANOVA ( $p \leq 0.05$ ). COD, chemical oxygen demand.

### 3. Results

#### 3.1. Impact of salinity on current production and physicochemical parameters

Salinity had a significant effect on electricity generation (Fig. 1a). Values of both electrochemical parameters were significantly greater in the control (CT) and low-salinity (LW) treatments compared to medium and high salinity treatments (ME and HG, respectively) during the experimental period. The HG treatment showed the lowest electricity production. Regardless of the salinity level, current production gradually increased after inoculation until day 24 of operation to remain unchanged towards the end of the experiment. No significant differences in the organic loading rate were observed in the influent for any of the treatments during the experimental period (Fig. 1b). Salinity had also a significant effect on the organic removal rate (Fig. 1c). The use of LW showed significantly greater values of organic removal rate ( $75\% \pm 2.1$ ) compared to CT ( $66\% \pm 1.4$ ), ME ( $58\% \pm 2.2$ ), and HG ( $42\% \pm 2.4$ ) treatments by day 30 of operation. Regardless of the treatment, values of CE gradually increased with time and were in the range of 15.8–19.3% towards the end of the experimental period (Fig. 1d).

A summary of changes in COD, suspended solids,  $\text{NH}_4^+\text{-N}$ , and  $\text{NO}_3^- \text{-N}$  concentrations, and values of conductivity and pH in the influents and effluents during the experimental period is provided in Table S3. No significant differences in the N removal % were observed between treatments with values ranging from 12 to  $25\% \pm 4.3$  during the experimental period. Salinity had no significant impact on the pH values and concentration of suspended solids which remained in the range of  $7.5\text{--}7.8 \pm 0.3$  and  $12.2\text{--}22.7 \pm 6.5 \text{ mg L}^{-1}$  during the experiment, respectively. As expected, treatment had a significant effect on conductivity values which significantly increased with greater salinity.

#### 3.2. Impact of salinity on the abundance, diversity, and composition of the bacterial community based on amplicon sequencing data

No significant differences in the abundance of bacterial communities were detected in the influent samples during the experimental period (Fig. S2a). Salinity had a significant effect on the absolute abundance (Fig. S2b) and alpha diversity (Fig. S2c) of the bacterial community on the anode based on 16S rRNA gene amplicon sequencing. Regardless of the time point, the abundance, number of ASVs, and values of the Shannon index of the bacterial community were significantly greater in the CT and LW treatments compared to ME and HG. No significant differences in the abundance and alpha diversity of the bacterial community were observed between time points for the influent samples, nor between inoculum samples. Treatment, time point, and their interaction had a significant effect on the composition of the bacterial community (Fig. 2). The ME and HG samples clustered together whereas those from the CT and LW treatments formed a separate group. No differences in beta-diversity were observed between influent samples, nor between inoculum samples.

An overview of the composition of the bacterial community at the phylum and genus taxonomic levels based on 16S rRNA gene amplicon sequencing is presented in Fig. S3. Firmicutes ( $46.1\% \pm 4.2$ ) and Proteobacteria ( $27.4\% \pm 4.1$ ) were the major phyla in the influent samples whereas Proteobacteria was the dominant phylum in the inoculum samples ( $72.3\% \pm 4.3$ ). The anode microbiome was mainly formed by Proteobacteria ( $46.6\% \pm 9.6$ ), Bacteroidota ( $25.3\% \pm 6.6$ ), Actinobacteriota ( $11.6\% \pm 7.1$ ), and Firmicutes ( $10.4\% \pm 7.1$ ) across time points and treatments.

Significantly enriched and depleted genera based on amplicon sequencing data were identified after 30 days of operation between LW, ME, and HG treatments compared to CT (Fig. 3). Treatment with LW resulted in significant increases in the relative abundance of a group of 16 genera (e.g., *Ignavibacterium*, *Desulfovibrio*, and *Desulfomicrobium*) whereas only *FTLpost3* and *Anaerovorax* were depleted. The use of ME

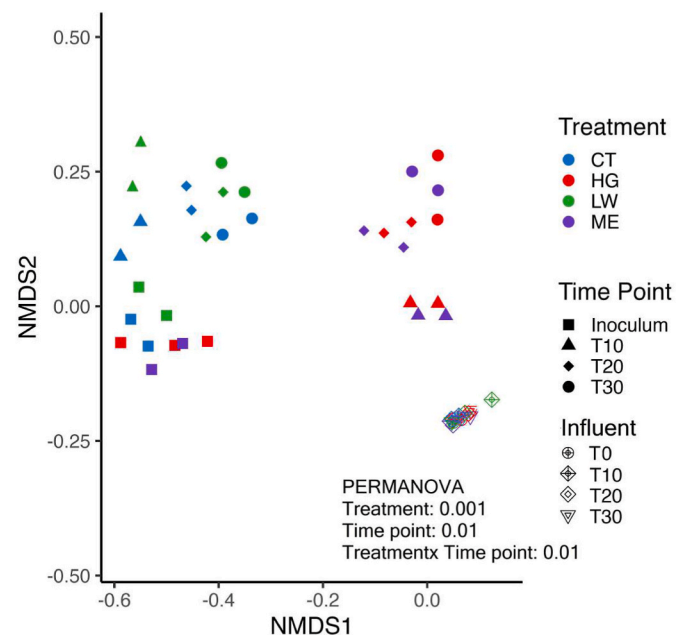


**Fig. 2.** Non-metric multidimensional scaling (NMDS) plots on unweighted UniFrac distances for the bacterial community during the experimental period for the different treatments. Differences in community composition between treatments, time points, and their interactions were tested by PERMANOVA. Stress = 0.124. Treatments are named as follows: CT, control; LW, low salinity; ME, medium salinity; HG, high salinity. Samples were taken after 0 (inoculum), 10 (T10), 20 (T20), and 30 days (T30). Samples from the influent are included.

treatment enriched taxa belonging to 7 genera (e.g., *Ignavibacterium*, *Desulfomicrobium*, and *Sphaerochaeta*) whereas the relative abundance of 4 genera (*Candidatus Competibacter*, *Lentimicrobium*, *Rikenellaceae*, and *Bact08*) was significantly reduced. Treatment with HG resulted in increases and decreases in the relative abundance of 24 (e.g., *Ignavibacterium*, *Desulfovibrio*, and *Fusibacter*) and 31 genera (e.g., *Dechlorobacter*, *Azovibrio*, and *Sedimentibacter*), respectively.

#### 3.3. Impact of salinity on the abundance and expression of genes belonging to different pathways and cycles

Variations in the functional and taxonomic profiles of selected cycles associated to different metabolic pathways were observed for the metagenomic (Fig. S4a and Fig. S4b, respectively) and metatranscriptomic (Fig. S5a and Fig. S5b, respectively) samples across treatments and time points. Regardless of the specific cycle, these variations were greater for the taxonomic than functional profiles, as revealed by ANOSIM analysis.

An overview of changes in the abundance and expression of genes belonging to different pathways within each of the cycles is provided in Table S4 and Table S5, respectively. Gradual increases in the abundance (Fig. 4a) and expression (Fig. 4b) of genes involved in iron reduction (EET genes) were observed for the CT and LW treatments after inoculation but they were reduced with greater salinity for the ME and HG treatments. The expression of genes involved in iron oxidation increased with greater salinity (Fig. 4b). The use of any salinity levels had no clear effect on gene transcripts for the iron storage and iron gene regulation pathways but the abundance of genes belonging to the latter pathway tended to increase with greater salinity (Fig. 4a and b).

Heatmaps showing variations in the abundance and expression of genes belonging to different pathways of each selected cycle are shown in Fig. S6 and Fig. S7, respectively. The abundance and expression of genes belonging to the Wood-Ljungdahl pathway of the carbon fixation cycle gradually increased with greater salinity compared to CT. The addition of any of the salinity levels increased the abundance and expression of genes within the Entner-Doudoroff pathway of the central

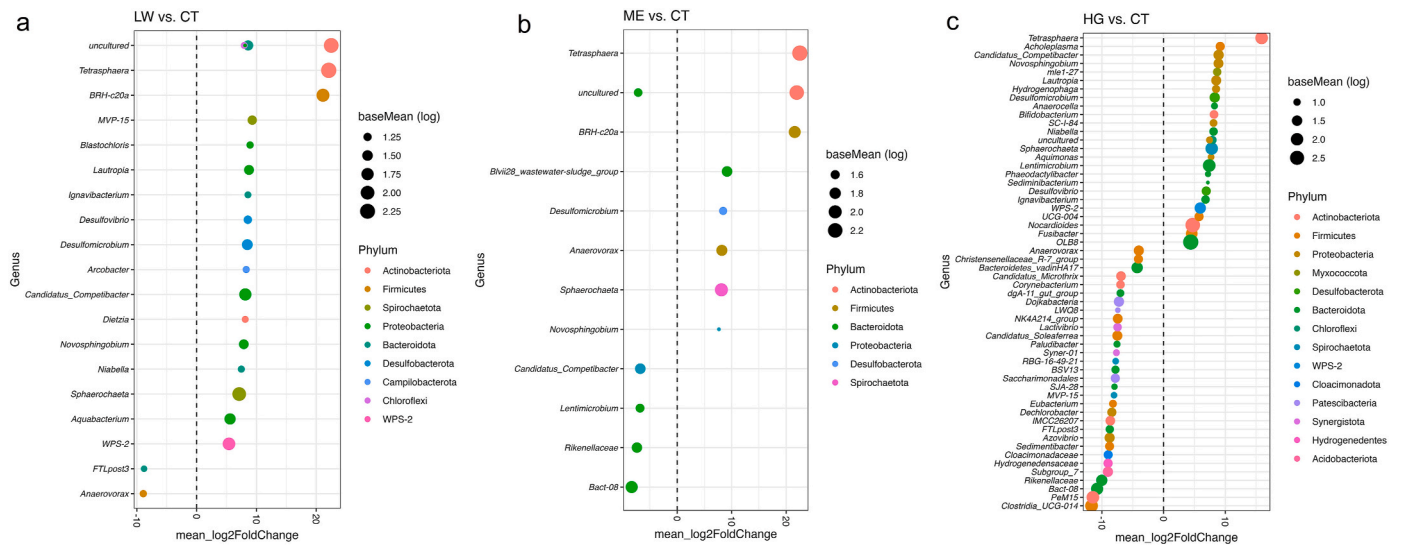


**Fig. 3.** Significantly enriched and depleted genera after 30 days of operation between LW (a), ME (b), and HG (c) treatments compared to CT according to DESeq2 analysis ( $p \leq 0.01$ ). Treatments are named as follows: CT, control; LW, low salinity; ME, medium salinity; HG, high salinity.

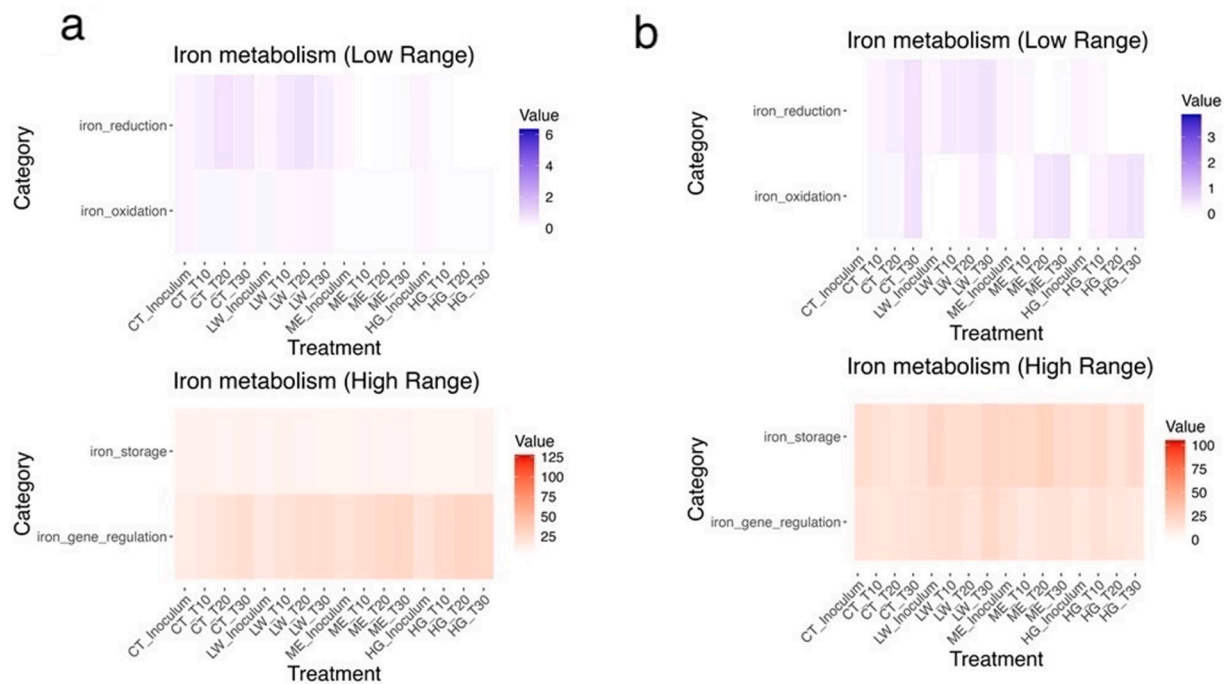


**Fig. 4.** Heatmaps showing variations in the abundance (a) and expression (b) of genes belonging to different pathways of the iron metabolism. RPKM and TPM values were used to construct the heatmaps, respectively. To enhance clarity and interpretability, the heat map has been divided into two panels: one representing the low range and the other representing the high range of the data. Treatments are named as follows: CT, control; LW, low salinity; ME, medium salinity; HG, high salinity. Samples were taken after 0 (inoculum), 10 (T10), 20 (T20), and 30 days (T30).

metabolism compared to CT, particularly for the ME and HG treatments. Increases in the expression of genes belonging to the mixed acid succinate pathway of fermentation were observed with greater salinity compared to CT. For the nitrogen metabolism, treatment with ME and HG produced decreases in the abundance and expression of the *nosZ* gene (involved in the reduction of nitrous oxide to dinitrogen) compared to LW and CT. Gene transcripts of *nirK* and *nirS* (involved in the reduction of nitrate to nitric oxide) were greater in the LW, ME, and HG treatments compared to CT but no differences among salinity levels were observed. The use of any of the saline treatments resulted in gradual increases in the expression of genes belonging to the thiosulfate

oxidation by SOX complex of the sulfur metabolism compared to CT. In addition, treatment with LW, ME, and HG resulted in gradual decreases and increases in the abundance of genes belonging to the sulfur dioxygenase and assimilatory sulfate reduction pathways, respectively, compared to CT. Salinity had no impact on the abundance and expression of genes involved in oxidative phosphorylation, methane metabolism, and pathways belonging to other general metabolisms. Increased salinity reduced gene transcripts belonging to the type VI secretion system. Gradual increases in the expression of genes associated with two-component systems of the phosphorus metabolism were observed with increased salinity compared to CT.

### 3.4. Metagenome community composition and taxonomic affiliation of genes involved in extra-cellular electron transfer

An overview of the microbial community composition at the kingdom and phylum taxonomic levels retrieved from the metagenomic samples is presented in Fig. S8. On average, Bacteria (98.2%  $\pm$  0.5) was the dominant kingdom across all treatments and time points. Slight increases (0.3–1.8%  $\pm$  0.6) in the relative abundance of archaea taxa were observed from inoculation to day 30 of operation, particularly in the CT treatment. Eukaryotes present in the inoculum (less than 3%  $\pm$  0.9) gradually disappear throughout the experimental period in all samples. On average, Proteobacteria (50.3%  $\pm$  17.4), Bacteroidota (15.9%  $\pm$  4.5), Actinobacteriota (12.4%  $\pm$  4.9), and Firmicutes (9.6%  $\pm$  5.8) were the dominant phyla across treatments and time points which agree with the amplicon sequencing analysis (section 3.2.) Regardless of the treatment, gradual increases in the relative abundance of taxa belonging to Firmicutes were observed with time, as also observed from data of the amplicon sequencing analysis (section 3.2.).

The taxonomic affiliation of EET genes was examined using EET genes annotated from metagenomic contigs. Outer membrane cytochromes (omc) and porin cytochromes (pc), and *OmcS* coding genes were selected for this analysis (Table S6). The outer membrane cytochromes (omc) and porin cytochromes (pc) coding genes were mainly associated to taxa belonging to the Ignavibacteria class and, to a lesser extent, to *Candidatus* Krumholzibacteriia (Table S7). The *omcS* gene originated from *Candidatus* Krumholzibacteria sp., *Acidobacteriota* sp., and *Gemmatimonas* sp. but taxa containing this gene were significantly lower (more than 12.5 times) in relative abundance compared to those with outer membrane cytochromes (omc) and porin cytochromes (pc) coding genes (Table S7).

### 3.5. Characterization of metagenome-assembled genomes with emphasis on those involved in extra-cellular electron transfer

A total of 893 MAGs were reconstructed out of which 263 had high quality (>90% complete and <5% contaminated). An overview of the taxonomic composition, completeness, contamination, and other general characteristic of the MAGs is provided in Table S8. Changes in the abundance of MAGs across time points and treatments for the metagenomic samples are shown in Table S9a, and changes in their transcript abundance are presented in Table S9b, respectively. We identified

fifteen MAGs containing at least one EET gene (Fig. 5). These represented 30 out of 45 iron reduction genes found in all contigs (including those contigs not binned into MAGs, Table S7), meaning that the EET MAGs were largely representative of the anode EET microbial community. *OmcS* was the only iron-reducing gene found in contigs but not binned, but these had a very low abundance compared to the genes found in the MAGs (Table S7). Linear mixed effects models revealed that all these MAGs significantly influence current production (Table 1). Heatmaps showing variations in the abundance and expression of EET genes and their associated MAGs across treatments and time points are presented in Fig. 5a and b, respectively. The heatmaps showed three main groups of EET and MAGs. The first group was formed by seven MAGs belonging to different genera (*UTCHB3*, *JAFDZ01*, *XYB12-FULL-38-5*, and *CAIKZJ01*) of the Ignavibacteriales and SJA-28 (*OLB5* genus) orders (Ignavibacteria class) and containing genes coding for outer membrane cytochromes (omc) and porin cytochromes (pc). For this first group of MAGs, the abundance and expression of the EET genes increased with time but it was always greater in the CT and LW treatments compared to ME and HG. A second group was formed by five MAGs classified as different genera (*JAIBA001*, *JAEUW101*, and *JAKJDA01*) of the Hydrogenedentiales order and containing genes coding for porin cytochromes (pc). For this second group of MAGs, the abundance and expression of the EET genes decreased with greater salinity (LW > ME > HG) and gradually increased during the experimental period only for the CT treatment. The third group was formed by three MAGs belonging to different genera (*UBA10908*, *UBA5559*, and *UBA1422*) of the Anaerovoracaceae family (Clostridia class) and containing Gram + EET genes *dmkA*, *dmkB*, *eetA*, *eetB*, *fmnB*, *ndh2*, and *pplA*. For this third group of MAGs, the abundance and expression of the EET slightly increased during the experimental period and was not affected by the salinity level. Overall, MAGs containing genes coding for outer membrane cytochromes and porin cytochromes were more abundant compared to the MAGs harboring Gram + EET genes (e.g., *dmkA*, *dmkB*, *eetA*, *eetB*, *fmnB*, *ndh2*, and *pplA*). A phylogenetic tree showing variations in the taxonomic affiliation of the MAGs containing EET genes is shown in Fig. S9. The tree shows that the MAGs were assigned to different species of the classes Ignavibacteria, Hydrogenedentia, and Clostridia.

Heatmaps showing variations in the mean abundance and transcription of the fifteen MAGs that contained at least one EET gene are shown in Fig. 6a and b, respectively. In general, the abundance of these MAGs was reduced in the ME and HG treatments compared to LW and

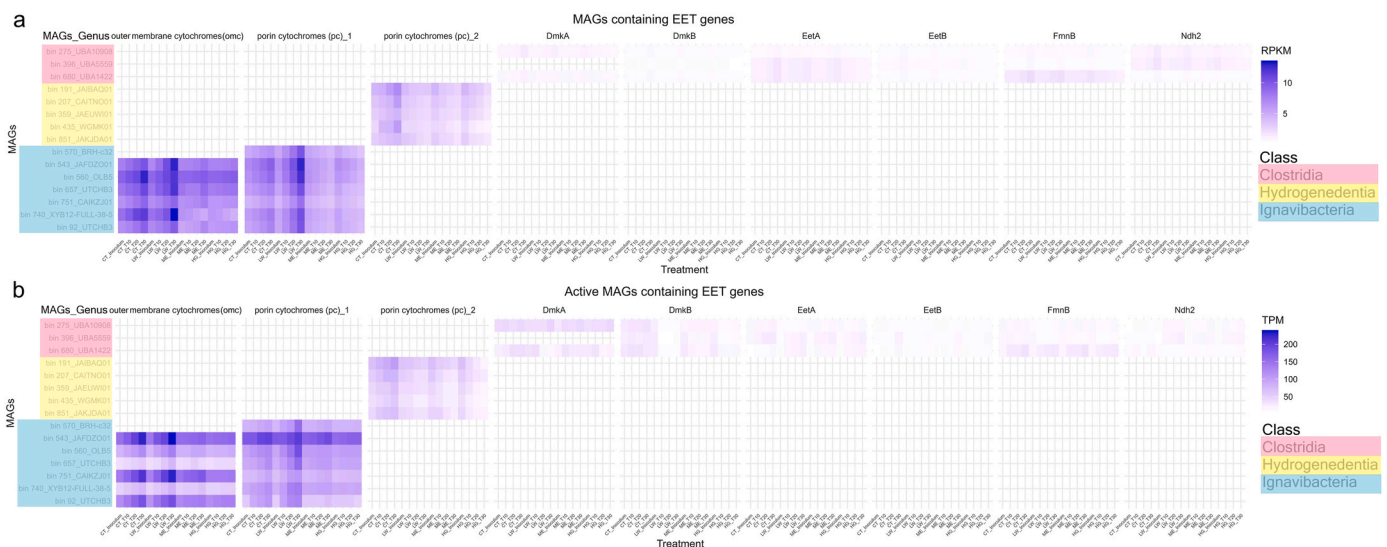


**Fig. 5.** Heatmaps showing changes in the abundance (a) and expression (b) of extra-cellular electron genes and their related MAGs across treatments and time points. Coverage and TPM values were used to construct the heatmaps, respectively. Taxonomic classification at the genus level is indicated for each MAG. Full taxonomic affiliation for the MAGs is provided in Table S8. Treatments are named as follows: CT, control; LW, low salinity; ME, medium salinity; HG, high salinity. Samples were taken after 0 (inoculum), 10 (T10), 20 (T20), and 30 days (T30).

**Table 1**

Statistical results of the linear mixed effects models for the active MAGs containing extra-cellular electron transfer genes as controllers of changes in current production. All linear models fulfilled the normal distribution of the residuals ( $p > 0.35$ , Shapiro's test). Significant codes:  $p < 0.05$ ,  $**p < 0.01$ ,  $***p < 0.001$ . The explained variance ( $R^2$ ) of each MAG was calculated as sums of squares for each variable  $\times 100$ /sums of squares for all MAGs. The coefficient estimate ( $\beta$ ) for each predictor is presented. Full taxonomic affiliation for the MAGs is provided in Table S8.

MAGs	Taxonomic affiliation	Current production		
		Coefficient estimates, $\beta$	Explained variance, $R^2$ (%)	Significance levels ( $p$ -value)
bin 92	Phylum Bacteroidota; Family Ignavibacteriaceae; Genus <i>UTCHB3</i>	0.83	9.31	***
bin 191	Phylum Hydrogenedentota; Family SLHB01; Genus <i>JAIBAQ01</i>	0.88	3.12	**
bin 207	Phylum Hydrogenedentota; Family CAITNO01	0.71	2.12	**
bin 275	Phylum Bacillota; Family Anaerovoracaceae; Genus <i>UBA10908</i>	0.79	1.85	*
bin 359	Phylum Hydrogenedentota; Family JAEUW101; Genus <i>JAEUW101</i>	0.72	3.77	**
bin 396	Phylum Bacillota; Family Anaerovoracaceae; Genus <i>UBA5559</i>	0.74	1.01	*
bin 435	Phylum Hydrogenedentota; Family WGMK01	0.79	3.56	**
bin 543	Phylum Bacteroidota; Family B-1AR; Genus <i>JAFDZ001</i>	0.92	7.43	***
bin 560	Phylum Bacteroidota; Family OLB5; Genus <i>OLB5</i>	0.84	7.65	***
bin 570	Phylum Bacteroidota; Family Melioribacteraceae; Genus <i>BRH-c32</i>	0.92	1.66	*
bin 657	Phylum Bacteroidota; Family Ignavibacteriaceae; Genus <i>UTCHB3</i>	0.88	8.92	***
bin 680	Phylum Bacillota; Family Anaerovoracaceae; Genus <i>UBA1422</i>	0.73	1.84	*
bin 740	Phylum Bacteroidota; Family Melioribacteraceae; Genus <i>XYB12-FULL-38-5</i>	0.84	9.03	***
bin 751	Phylum Bacteroidota; Family B-1AR; Genus <i>CAIKZJ01</i>	0.92	8.14	***
bin 851	Phylum Hydrogenedentota; Family SLHB01; Genus <i>JAKJDA01</i>	0.74	5.16	**

CT. MAGs such as 275 (*UBA0908* genus of the Anaerovoracaceae family), 543 (*JAFDZ001* genus of the B-1AR family), and 680 (*UBA1422* genus of the Anaerovoracaceae family) were particularly abundant in the LW treatments compared to the rest of the treatments. The abundance of the MAG 92 (*UTCHB3* genus of the Ignavibacteriaceae family) increased with greater salinity. The most active MAGs with EET genes

were 92 and 657 (*UTCHB3* genus), 207 (*CAITNO01* genus), and 560 (*OLB5* genus) but only MAG 657 was active in all treatments. Eleven of the fifteen MAGs that contained at least one EET gene also had genes encoding for  $\text{Na}^+/\text{H}^+$  antiporters (e.g., *nhaA*, *nhaB*, *nhaC*, *nhaP*, *mnhA*, or *mnpA* genes) (Table S10). The rest of the MAGs had genes encoding for  $\text{K}^+/\text{H}^+$  antiporters and other compatible solutes such as betaine, trehalose, and sucrose.

#### 4. Discussion

We found that the salinity level of urban wastewater determines changes in the abundance and expression of EET genes, impacting electricity generation in a continuous-flow MFC. The use of low salinity (3.5 g/L of NaCl) resulted in greater current production and organic removal efficiency compared to medium and high salinity treatments (7 and 15 g/L of NaCl, respectively), and the untreated control. The beneficial effect of the low salinity level on electricity generation was linked to increased abundance and activity of electroactive microorganisms. Taxa belonging to the Ignavibacteria class and containing genes coding for outer membrane cytochromes (omc) and porin cytochromes (pc) were the main electroactive microorganisms in the anode biofilm, and their abundance and activity were favored under low salinity level. Electroactive MAGs showed mechanisms for salt-tolerance such  $\text{Na}^+/\text{H}^+$  antiporters and other biosynthetic pathways for osmotic solutes. Salinity level also determined variations in the abundance, and alpha- and beta-diversity of bacterial communities with medium and high salinity limiting bacterial growth. Together, our findings have important environmental and bioengineering implications as they show that certain exoelectrogens can thrive in low salinity conditions, enhancing treatment performance and electricity generation of MFCs treating saline urban wastewater. This knowledge contributes to improving our understanding of salinity impacts on EET genes and can help select optimal salinity conditions in MFCs treating real effluents. Although previous research has demonstrated the potential of saline wastewater to support power generation in MFCs most of these studies were run in MFCs under fed-batch mode for limited periods of time and were fed with synthetic medium simulating real wastewater (Lefebvre et al., 2006, 2012; Li et al., 2013; Guo et al., 2021; Saravanan et al., 2023). Here, we used a continuous-flow MFC fed with real urban wastewater, which contains more complex carbon sources than synthetic media and may determine variations in anode colonization, microbial community composition, and subsequent current production, as supported by our results. Continuous-flow MFCs are more suitable for practical applications compared to batch-mode MFCs as they can treat larger volumes for longer periods of time (Chung et al., 2009; Cai et al., 2014; Cabrera et al., 2022). Therefore, our results may aid in scaling up MFCs for treating saline effluents.

##### 4.1. Salinity impacts on electrochemical performance and electroactive microorganisms

The low salinity level enhanced energy generation compared to medium and high treatments, an effect that was related to increased abundance and expression of EET genes. The taxonomic affiliation of EET genes coding for outer membrane cytochromes (omc) and porin cytochromes (pc) was dominated by taxa belonging to the Ignavibacteria class. Genera belonging to this class have been found in a variety of environments (Podosokorskaya et al., 2023) including MFCs inoculated with activated sludge from WWTPs and fed with synthetic wastewater (Yoshizawa et al., 2014; Ding et al., 2017). For example, *Ignavibacterium* sp. has been reported to contain porin cytochromes (pc)-coding genes (Shi et al., 2014). Here, we extend this previous work by showing not only the presence and active role of Ignavibacteria-associated genera for EET in an MFC fed with saline wastewater but also its ability to adapt to different salinity conditions likely due to the presence of genes encoding for  $\text{Na}^+/\text{H}^+$  antiporters. The study of the diversity of electroactive taxa

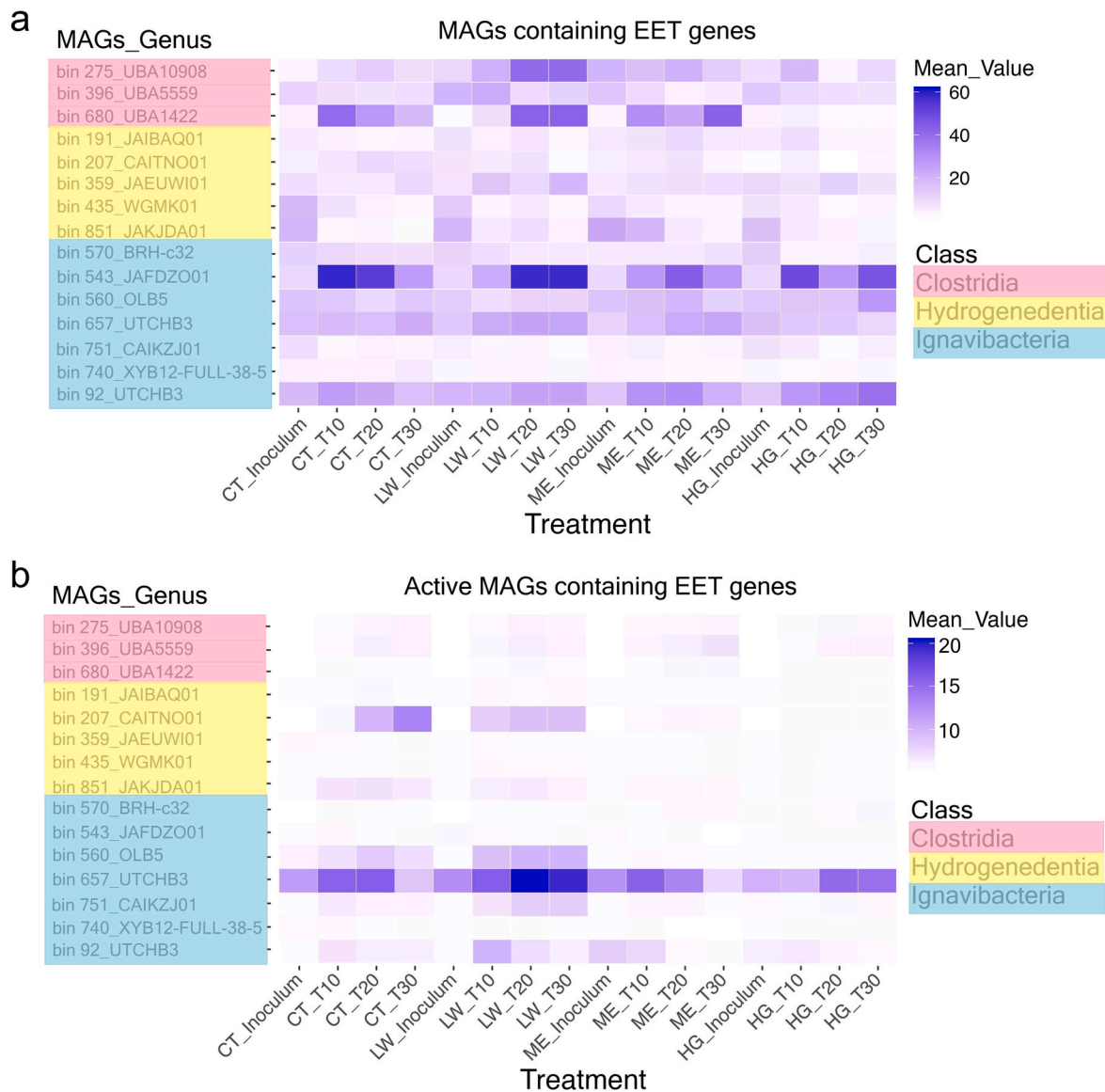


**Fig. 6.** Heatmaps showing changes in the abundance of MAGs containing extra-cellular electron genes across treatments and time points for the metagenomic (a) and metatranscriptomic (b) samples. Coverage and TPM values were used to construct the heatmaps, respectively. Taxonomic classification at the genus level is indicated for each MAG. Full taxonomic affiliation for the MAGs is provided in [Table S8](#). Treatments are named as follows: CT, control; LW, low salinity; ME, medium salinity; HG, high salinity. Samples were taken after 0 (inoculum), 10 (T10), 20 (T20), and 30 days (T30).

containing outer membrane cytochromes (*omc*) and porin cytochromes (*pc*) also showed that they were Gram-negative bacteria, which aligns well with previous work on microorganisms having mechanisms that can shuttle electrons across an outer membrane ([Wrighton et al., 2011](#); [Paquete et al., 2022](#); [Lovley and Holmes, 2021](#)).

We identified fifteen MAGs containing EET genes that were significantly correlated with improved current production. These MAGs were associated to 3 classes (Ignavibacteria, Hydrogenedentia, and Clostridia) and 15 different genera thus showing that activated sludge from WWTPs can harbor a diverse group of exoelectrogens able to colonize anodes in MFCs fed with saline effluents. All the 15 MAGs exhibited differential gene expression influenced by the salinity levels. For example, Ignavibacteria-associated MAGs containing genes coding for outer membrane cytochromes (*omc*) and porin cytochromes (*pc*) were favored under low salinity levels compared to the rest of the treatments. Other taxa affiliated to Hydrogenedentia class and containing genes coding for porin cytochromes (*pc*) decreased with increased salinity. The potential role of Hydrogenedentia strains in the current generation of MFCs

remains largely unknown. MAGs affiliated with the Anaerovoraceae family (Clostridia class) consistently expressed EET genes such as *dmkA*, *dmkB*, *eetA*, *eetB*, *fmnB*, *ndh2*, and *pplA*, regardless of salinity conditions. Members of the Anaerovoraceae family such as *Clostridium* are known electroactive microorganisms ([Logan et al., 2019](#)). However, the consistent expression of *dmkA*, *dmkB*, *eetA*, *eetB*, *fmnB*, *ndh2*, and *pplA* genes implies that members of the Anaerovoraceae family possess adaptive capabilities that allow them to maintain EET under both moderate and high salinity levels. It is interesting to note that eleven of the fifteen MAGs containing EETs had genes encoding for  $\text{Na}^+/\text{H}^+$  antiporters (e.g., *nhaA*, *nhaB*, *nhaC*, *nhaP*, *mnhA*, or *mrpA* genes) confirming the presence of mechanisms for salt tolerance in these exoelectrogens which can explain their survival in saltwater environments such as our MFC system. The other four MAGs belonged to the genera *JAI-BAQ01*, *UTCHB3*, *BRH-c32*, and *OLB5* and had genes encoding for  $\text{K}^+/\text{H}^+$  antiporters and other compatible solutes such as betaine, trehalose, and sucrose which may also help to tolerate salinity.

Overall, our results suggest that salinity induces increases in the

relative abundance of Gram-negative bacteria of the Ignavibacteria class (seven out of 15 MAGs) harboring EET genes coding for outer membrane cytochromes (omc) and porin cytochromes (pc). However, we also detected the presence of Gram-positive bacteria (genera associated to the Hydrogenedentia class and Anaerovoracaceae family) as exoelectrogens in our system. These results highlight that diverse mechanisms for EET from Gram-negative and Gram-positive taxa are present in the anode biofilm of an MFC fed with saline wastewater. Although salinity influenced the composition and functional potential of the microbial community, qPCR analysis showed that the overall microbial biomass in the influent remained unchanged across treatments. This suggests that shifts in electroactive community composition and abundance were driven by salinity-induced selection rather than changes in total microbial abundance. The stability in biomass could be explained by a dynamic replacement of microorganisms without affecting the total cell number, possible constraints in nutrient availability limiting overall growth, microbial stress responses that allow survival under different salinity conditions without significant population loss, or a combination of these factors. Additionally, biofilm formation dynamics may play a role, as microbial communities often reach a structural equilibrium where total biomass remains stable, limited by the available surface area, despite shifts in community composition.

In addition to improving the current generation, we found that the low salinity level enhanced organic removal efficiency (COD removal of 75% with HRT of 1 day) compared to medium and high treatments. Previous studies have shown similar COD removal of 84% (initial concentration of 1.21 g COD/L) at an HRT of 20 days in a MFC inoculated with halophilic microbial consortia and treating saline wastewater (Guo et al., 2021; Jamal and Pugazhendi, 2021). The detrimental effect of ME and high HG treatments on COD removal could be due to ionic toxicity affecting bacterial growth, as also shown by the significantly lower abundance and alpha diversity of bacterial communities in the anode biofilm compared to the LW treatment. Nevertheless, the coulombic efficiency was similar among salinity levels and reached values close to 20% by the end of the experiment. These results suggest that there were other electron sinks in the anode (e.g., denitrification and methanogenesis; Fig. S6) limiting efficient electron transfer. In addition, the lack of changes in coulombic efficiency between the salinity treatments suggests that the non-anode-reducing community was as affected by salinity as the anode-reducing community.

The amplicon sequencing analysis revealed that salinity significantly influences the diversity and composition of the anode biofilm microbiome, shaping the structure of the microbial communities colonizing the electrode. Alpha diversity varied across treatments, with significantly higher values in the LW treatment compared to ME and HG, indicating that lower salinity levels supported a more diverse microbial community. The greater alpha diversity observed in LW likely facilitated the establishment of a robust electroactive community, enhancing EET and leading to improved current production. This higher diversity may contribute to improved functional redundancy and resilience, which are critical for maintaining electrochemical performance under fluctuating environmental conditions. Beta-diversity analyses indicated that the microbial communities in the anode biofilm were significantly structured by salinity level, with distinct clustering of LW and HG treatments, suggesting that osmotic stress played a key role in determining microbial composition. The use of low salinity favored increases in the abundance of genera known for having electroactive microbes such as *Ignavibacterium*, *Desulfovibrio*, and *Desulfomicrobium* (Logan et al., 2019). Medium and particularly high salinity treatments produced decreases in the relative abundance of specific and numerous bacterial genera (e.g., *Dechlorobacter*, *Azovibrio*, and *Sedimentibacter*) but other microorganisms (e.g., *Desulfovibrio* and *Fusibacter*) were tolerant to these saline conditions. Together, these results suggest that variations in the composition of bacterial communities in the anode biofilm were likely due to differences in the tolerance to osmotic stress between microorganisms, ultimately influencing MFC treatment performance and energy

generation. Of note, we found that *Ignavibacterium* adapted well from low to high salinity levels which agrees with metagenomic and meta-transcriptomic data, and again points towards members of this class as exoelectrogens and able to adapt to varying salinity conditions in MFCs.

The study of the impact of salinity on other general metabolisms showed differential responses of microbial genes to salinity highlighting the complex interplay between salinity stress and microbial metabolic adaptation (see Note S1). Variations in various microbial strategies known to cope with salinity were observed in the anode microbiome, including adjustments in metabolic pathways, stress response mechanisms, and shifts in microbial community composition (see Note S1). These adaptations may directly or indirectly influence EET by affecting microbial energy production, redox balance, and electron donor availability, ultimately shaping the efficiency of current generation and organic matter removal in the system (see Note S1).

#### 4.2. Implications for bioengineering applications

The bioengineering implications of our findings are significant, particularly for the design and optimization of MFCs in environments with variable salinity, such as coastal urban WWTPs or saline effluents from industry. In addition to demonstrating practical bioengineering strategies, this study makes novel contributions by using continuous-flow MFCs with real urban wastewater, in contrast to previous research that relied on batch-mode systems or synthetic media. This allows for a more realistic evaluation of microbial community dynamics and their response to different salinity levels, providing insights critical for scaling up MFC technologies. In particular, our study shows that low levels of salinity can increase the electrochemical performance of MFCs treating real wastewater. Yet, future studies should explore how MFC technology could be integrated with complementary treatment technologies, such as anaerobic digestion, constructed wetlands, or advanced oxidation processes, to further enhance wastewater treatment efficiency and energy recovery (Dwivedi et al., 2022; Feng et al., 2024). Such hybrid systems could leverage the synergistic effects of different microbial and electrochemical processes, improving overall contaminant removal while maximizing bioelectricity generation.

The identification of diverse exoelectrogens in our study, including both Gram-negative (Ignavibacteria) and Gram-positive (Clostridia) taxa, demonstrates the breadth of microbial mechanisms contributing to electron transfer. This diversity, along with the discovery of EET genes linked to salt-tolerance mechanisms, suggests potential strategies for engineering more resilient MFC systems capable of maintaining high efficiency across a range of environmental conditions.

The ability of Ignavibacteria to maintain and even enhance EET gene expression at lower salinity levels suggests that bioengineering strategies targeting specific microbial communities could enhance both treatment performance and energy recovery. These findings also point to the potential for selectively enriching electroactive microbial populations in MFC systems to optimize performance under specific environmental conditions. Furthermore, the salinity-induced shifts in the microbial community composition, with higher salinity levels limiting microbial growth and diversity, emphasize the need for careful control of salinity in bioelectrochemical systems. The decline in microbial diversity at higher salinity levels may be linked to the inhibition of key metabolic pathways beyond EET, as indicated by the reduced abundance of genes involved in nitrogen metabolism and other general microbial functions. This underscores the complex interplay between salinity stress and microbial metabolic adaptation, further reinforcing the importance of optimizing salinity for enhanced MFC performance.

#### 5. Conclusions

This study shows that salinity levels play a critical role in determining the performance and electricity generation of continuous-flow MFCs treating real urban wastewater by altering exoelectrogens and

other microorganisms of the anode microbiome. Our findings demonstrate that lower salinity levels (3.5 g/L NaCl) enhance electricity generation and organic removal efficiency, while higher salinity levels (7 and 15 g/L NaCl) constrain microbial growth and diversity, ultimately limiting electrochemical performance. These results emphasize the critical role of microbial adaptation in shaping the functionality of MFCs under varying salinity conditions. An increase in the abundance and activity of certain electroactive microorganisms, particularly those within the Ignavibacteria class, highlights the ability of anode microbiome members to adapt to salinity conditions. This adaptation is linked to the presence of outer membrane cytochromes and porin cytochromes and mechanisms for salt-tolerance encoded in their genomes. This research provides valuable insights into the interplay between salinity stress and microbial adaptation, contributing to the optimization and scale-up of MFC technologies for enhanced environmental and bioengineering applications using real effluents.

### CRedit authorship contribution statement

**Antonio Castellano-Hinojosa:** Writing – review & editing, Writing – original draft, Visualization, Investigation, Funding acquisition, Data curation, Conceptualization. **Manuel J. Gallardo-Altamirano:** Writing – review & editing, Investigation, Conceptualization. **Clementina Pozo:** Writing – review & editing, Investigation, Conceptualization. **Alejandro González-Martínez:** Writing – review & editing, Investigation, Conceptualization. **Jesús González-López:** Writing – review & editing, Investigation, Funding acquisition, Conceptualization. **Ian P.G. Marshall:** Writing – review & editing, Visualization, Investigation, Data curation, Conceptualization.

### Declaration of competing interest

The authors declare that they have no known competing financial interests or personal relationships that could have appeared to influence the work reported in this paper.

### Acknowledgments

This research was financially supported by the Marie Skłodowska-Curie Postdoctoral European Fellowship (101108081) from HORIZON-MSCA-2022-PF-01 (Horizon Europe, 2022). Most of the computing for this project was performed on the GenomeDK cluster. We would like to thank GenomeDK and Aarhus University for providing computational resources and support that contributed to these research results.

### Appendix A. Supplementary data

Supplementary data to this article can be found online at <https://doi.org/10.1016/j.jenvman.2025.124858>.

### Data availability

Data will be made available on request.

### References

- Alam, R., Khan, S.U., Usman, M., Asif, M., Farooqi, I.H., 2022. A critical review on treatment of saline wastewater with emphasis on electrochemical based approaches. *Process Saf. Environ. Prot.* 158, 625–643. <https://doi.org/10.1016/j.psep.2021.11.054>.
- Andrews, S., 2010. FastQC: a quality control tool for high throughput sequence data. <https://www.bioinformatics.babraham.ac.uk/projects/fastqc/>.
- APHA, 2012. Standard Methods for the Examination of Water and Wastewater. American Public Health Association, Washington, DC, USA. <https://doi.org/10.1100/2012/462467>.
- Aramaki, T., Blanc-Mathieu, R., Endo, H., Ohkubo, K., Kanehisa, M., Goto, S., Ogata, H., 2020. KofamKOALA: KEGG Ortholog assignment based on profile HMM and adaptive score threshold. *Bioinformatics* 36, 2251–2252. <https://doi.org/10.1093/bioinformatics/btz859>.

- Baker, I.R., Conley, B.E., Gralnick, J.A., Girguis, P.R., 2022. Evidence for horizontal and vertical transmission of Mtr-mediated extracellular electron transfer among the bacteria. *mBio* 13. <https://doi.org/10.1128/MBIO.02904-21/ASSET/E268C30E-DC75-4B73-BFAF-57C2F91458D6/ASSETS/IMAGES/MEDIUM/MBIO.02904-21-F007.GIF>.
- Bates, D., Mächler, M., Bolker, B.M., Walker, S.C., 2015. Fitting linear mixed-effects models using lme4. *J. Stat. Softw.* 67, 1–48. <https://doi.org/10.18637/jss.v067.i01>.
- Bolger, A.M., Lohse, M., Usadel, B., 2014. Trimmomatic: a flexible trimmer for Illumina sequence data. *Bioinformatics* 30, 2114–2120. <https://doi.org/10.1093/bioinformatics/btu170>.
- Bolyen, E., Rideout, J.R., Dillon, M.R., Bokulich, N.A., Abnet, C.C., Al-Ghalith, G.A., Alexander, H., Alm, E.J., Arumugam, M., Asnicar, F., Bai, Y., Bisanz, J.E., Bittinger, K., Brejnrod, A., Brislawn, C.J., Brown, C.T., Callahan, B.J., Caraballo-Rodríguez, A.M., Chase, J., Cope, E.K., Da Silva, R., Diener, C., Dorrestein, P.C., Douglas, G.M., Durall, D.M., Duvallet, C., Edwardson, C.F., Ernst, M., Estaki, M., Fouquier, J., Gauglitz, J.M., Gibbons, S.M., Gibson, D.L., Gonzalez, A., Gorlick, K., Guo, J., Hillmann, B., Holmes, S., Holste, H., Huttenhower, C., Huttley, G.A., Janssen, S., Jarmusch, A.K., Jiang, L., Kaehler, B.D., Kang, K., Kang, K., Keefe, C.R., Keim, P., Kelley, S.T., Knights, D., Koester, I., Kosciolk, T., Kreps, J., Langille, M.G. I., Lee, J., Ley, R., Liu, Y.X., Loftfield, E., Lozupone, C., Maher, M., Marotz, C., Martin, B.D., McDonald, D., McIver, L.J., Melnik, A.V., Metcalf, J.L., Morgan, S.C., Morton, J.T., Naimy, A.T., Navas-Molina, J.A., Nothias, L.F., Orchanian, S.B., Pearson, T., Peoples, S.L., Petras, D., Preuss, M.L., Pruesse, E., Rasmussen, L.B., Rivers, A., Robeson, M.S., Rosenthal, P., Segata, N., Shaffer, M., Shiffer, A., Sinha, R., Song, S.J., Spear, J.R., Swafford, A.D., Thompson, L.R., Torres, P.J., Trinh, P., Tripathi, A., Tumbaugh, P.J., Ul-Hasan, S., van der Hooft, J.J.J., Vargas, F., Vázquez-Baeza, Y., Vogtmann, E., von Hippel, M., Walters, W., Wan, Y., Wang, M., Warren, J., Weber, K.C., Williamson, C.H.D., Willis, A.D., Xu, Z.Z., Zaneveld, J.R., Zhang, Y., Zhu, Q., Knight, R., Caporaso, J.G., 2019. Reproducible, interactive, scalable and extensible microbiome data science using QIIME 2. *Nat. Biotechnol.* 37(8), 852–857. <https://doi.org/10.1038/s41587-019-0209-9>, 2019.
- Cabrera, J., Dai, Y., Irfan, M., Li, Y., Gallo, F., Zhang, P., Zong, Y., Liu, X., 2022. Novel continuous up-flow MFC for treatment of produced water: flow rate effect, microbial community, and flow simulation. *Chemosphere* 289, 133186. <https://doi.org/10.1016/j.chemosphere.2021.133186>.
- Cai, J., Zheng, P., Qaisar, M., Xing, Y., 2014. Effect of operating modes on simultaneous anaerobic sulfide and nitrate removal in microbial fuel cell. *J. Ind. Microbiol. Biotechnol.* 41, 795–802. <https://doi.org/10.1007/S10295-014-1425-4>.
- Cai, T., Zhang, Y., Wang, N., Zhang, Z., Lu, X., Zhen, G., 2022. Electrochemically active microorganisms sense charge transfer resistance for regulating biofilm electroactivity, spatio-temporal distribution, and catabolic pathway. *Chem. Eng. J.* 442, 136248. <https://doi.org/10.1016/j.cej.2022.136248>.
- Callahan, B.J., McMurdie, P.J., Rosen, M.J., Han, A.W., Johnson, A.J.A., Holmes, S.P., 2016. DADA2: high-resolution sample inference from Illumina amplicon data. *Nat. Methods* 137, 581–583. <https://doi.org/10.1038/nmeth.3869>, 2016.
- Camacho, C., Coulouris, G., Avagyan, V., Ma, N., Papadopoulos, J., Bealer, K., Madden, T.L., 2009. BLAST+: architecture and applications. *BMC Bioinf.* 10, 1–9. <https://doi.org/10.1186/1471-2105-10-421/FIGURES/4>.
- Castellano-Hinojosa, A., González-Martínez, A., Pozo, C., González-López, J., 2022. Diversity of electroactive and non-electroactive microorganisms and their potential relationships in microbial electrochemical systems: a review. *J. Water Process Eng.* 50, 103199. <https://doi.org/10.1016/j.jwpe.2022.103199>.
- Castellano-Hinojosa, A., Albrecht, U., Strauss, S.L., 2023. Interactions between rootstocks and compost influence the active rhizosphere bacterial communities in citrus. *Microbiome* 11, 1–16. <https://doi.org/10.1186/S40168-023-01524-Y/FIGURES/6>.
- Castellano-Hinojosa, A., Gallardo-Altamirano, M.J., Pozo, C., González-Martínez, A., González-López, J., 2024. Hydraulic retention time drives changes in energy production and the anodic microbiome of a microbial fuel cell (MFC). *J. Water Process Eng.* 59, 104966. <https://doi.org/10.1016/j.jwpe.2024.104966>.
- Castellano-Hinojosa, A., Gallardo-Altamirano, M.J., Pozo, C., González-Martínez, A., González-López, J., 2025. Inoculum selection and hydraulic retention time impacts in a microbial fuel cell treating saline wastewater. *Appl. Microbiol. Biotechnol.* 109, 29. <https://doi.org/10.1007/s00253-024-13377-y>.
- Chaumeil, P.A., Mussig, A.J., Hugenholtz, P., Parks, D.H., 2022. GTDB-Tk v2: memory friendly classification with the genome taxonomy database. *Bioinformatics* 38, 5315–5316. <https://doi.org/10.1093/BIOINFORMATICS/BTAC672>.
- Chklovskii, A., Parks, D.H., Woodcroft, B.J., Tyson, G.W., 2023. CheckM2: a rapid, scalable and accurate tool for assessing microbial genome quality using machine learning. *Nat. Methods* 208, 1203–1212. <https://doi.org/10.1038/s41592-023-01940-w>, 2023.
- Chung, K., Okabe, S., 2009. Continuous power generation and microbial community structure of the anode biofilms in a three-stage microbial fuel cell system. *Appl. Microbiol. Biotechnol.* 83, 965–977. <https://doi.org/10.1007/S00253-009-1990-Z/FIGURES/8>.
- Correa-Galeote, D., Roibás, A., Mosquera-Corral, A., Juárez-Jiménez, B., González-López, J., Rodelas, B., 2021. Salinity is the major driver of the global eukaryotic community structure in fish-canning wastewater treatment plants. *J. Environ. Manage.* 290, 112623. <https://doi.org/10.1016/j.jenvman.2021.112623>.
- Cortés-Lorenzo, C., Rodríguez-Díaz, M., Sipkema, D., Juárez-Jiménez, B., Rodelas, B., Smidt, H., González-López, J., 2015. Effect of salinity on nitrification efficiency and structure of ammonia-oxidizing bacterial communities in a submerged fixed bed bioreactor. *Chem. Eng. J.* 266, 233–240. <https://doi.org/10.1016/j.cej.2014.12.083>.

- Ding, J., Lu, Y.Z., Fu, L., Ding, Z.W., Mu, Y., Cheng, S.H., Zeng, R.J., 2017. Decoupling of DAMO archaea from DAMO bacteria in a methane-driven microbial fuel cell. *Water Res.* 110, 112–119. <https://doi.org/10.1016/j.watres.2016.12.006>.
- Dwivedi, K.A., Huang, S.-J., Wang, C.-T., 2022. Integration of various technology-based approaches for enhancing the performance of microbial fuel cell technology: a review. *Chemosphere* 287, 132248. <https://doi.org/10.1016/j.chemosphere.2021.132248>.
- Egea-Corbacho, A., Romero-Pareja, P., Aragón Cruz, C., Pavón, C., Coello, M.D., 2021. Effect of seawater intrusion using real wastewater on an attached biomass system operating a nitrogen and phosphorus removal process. *J. Environ. Chem. Eng.* 9, 104927. <https://doi.org/10.1016/j.jece.2020.104927>.
- Feng, F., Wu, C.-H., Li, F., Wang, X., Zhu, J., Zhang, R., Chen, S.-C., 2024. Research on the integration of microbial fuel cells with conventional wastewater treatment technology: advantages of anaerobic fermentation. *Energy Convers. Manag.* X 23, 100680. <https://doi.org/10.1016/j.ecmx.2024.100680>.
- Fortunato, C.S., Crump, B.C., 2015. Microbial gene abundance and expression patterns across a river to ocean salinity gradient. *PLoS One* 10, e0140578. <https://doi.org/10.1371/JOURNAL.PONE.0140578>.
- Garber, A.I., Neelson, K.H., Okamoto, A., McAllister, S.M., Chan, C.S., Barco, R.A., Merino, N., 2020. FeGenie: a comprehensive tool for the identification of iron genes and iron gene neighborhoods in genome and metagenome assemblies. *Front. Microbiol.* 11, 499513. <https://doi.org/10.3389/fmicb.2020.00037/BIBTEX>.
- Gruber-Vodicka, H.R., Seah, B.K.B., Pruesse, E., 2020. phyloFlash: rapid small-subunit rRNA profiling and targeted assembly from metagenomes. *mSystems* 5. [https://doi.org/10.1128/MSYSTEMS.00920-20/SUPPL\\_FILE/REVIEWER-COMMENTS.PDF](https://doi.org/10.1128/MSYSTEMS.00920-20/SUPPL_FILE/REVIEWER-COMMENTS.PDF).
- Guo, F., Luo, H., Shi, Z., Wu, Y., Liu, H., 2021. Substrate salinity: a critical factor regulating the performance of microbial fuel cells, a review. *Sci. Total Environ.* 763, 143021. <https://doi.org/10.1016/j.scitotenv.2020.143021>.
- He, H., Chen, Y., Li, X., Cheng, Y., Yang, C., Zeng, G., 2017. Influence of salinity on microorganisms in activated sludge processes: a review. *Int. Biodeterior. Biodegradation* 119, 520–527. <https://doi.org/10.1016/j.ibiod.2016.10.007>.
- Hyatt, D., Chen, G.L., LoCascio, P.F., Land, M.L., Larimer, F.W., Hauser, L.J., 2010. Prodigal: prokaryotic gene recognition and translation initiation site identification. *BMC Bioinform.* 11, 1–11. <https://doi.org/10.1186/1471-2105-11-119/TABLES/5>.
- Ishii, S., Suzuki, S., Norden-Krichmar, T.M., Tenney, A., Chain, P.S.G., Scholz, M.B., Neelson, K.H., Bretschger, O., 2013. A novel metatranscriptomic approach to identify gene expression dynamics during extracellular electron transfer. *Nat. Commun.* 4(1), 1–10. <https://doi.org/10.1038/ncomms2615>, 2013.
- Jamal, M.T., Pugazhendhi, A., 2021. Treatment of fish market wastewater and energy production using halophiles in air cathode microbial fuel cell. *J. Environ. Manage.* 292, 112752. <https://doi.org/10.1016/j.jenvman.2021.112752>.
- Ji, X.M., Wang, Y.L., Zhan, X., Wu, Z., Lee, P.H., 2022. Meta-Omics reveal the metabolic acclimation of freshwater anaerobic bacteria for saline wastewater treatment. *J. Clean. Prod.* 362, 132184. <https://doi.org/10.1016/j.jclepro.2022.132184>.
- Kang, D.D., Li, F., Kirton, E., Thomas, A., Egan, R., An, H., Wang, Z., 2019. MetaBAT 2: an adaptive binning algorithm for robust and efficient genome reconstruction from metagenome assemblies. *PeerJ*. <https://doi.org/10.7717/PEERJ.7359/SUPP-3>, 2019.
- Kim, Y., Logan, B.E., 2013. Simultaneous removal of organic matter and salt ions from saline wastewater in bioelectrochemical systems. *Desalination* 308, 115–121. <https://doi.org/10.1016/j.desal.2012.07.031>.
- Koch, C., Harnisch, F., 2016. Is there a specific ecological niche for electroactive microorganisms? *Chemelectrochem* 3, 1282–1295. <https://doi.org/10.1002/CELC.201600079>.
- Lefebvre, O., Moletta, R., 2006. Treatment of organic pollution in industrial saline wastewater: a literature review. *Water Res.* 40, 3671–3682. <https://doi.org/10.1016/j.watres.2006.08.027>.
- Lefebvre, O., Tan, Z., Kharkwal, S., Ng, H.Y., 2012. Effect of increasing anodic NaCl concentration on microbial fuel cell performance. *Bioresour. Technol.* 112, 336–340. <https://doi.org/10.1016/j.biortech.2012.02.048>.
- Li, H., Handsaker, B., Wysoker, A., Fennell, T., Ruan, J., Homer, N., Marth, G., Abecasis, G., Durbin, R., 2009. The sequence alignment/map format and SAMtools. *Bioinformatics* 25, 2078. <https://doi.org/10.1093/BIOINFORMATICS/BTP352>.
- Li, X.M., Cheng, K.Y., Wong, J.W.C., 2013. Bioelectricity production from food waste leachate using microbial fuel cells: effect of NaCl and pH. *Bioresour. Technol.* 149, 452–458. <https://doi.org/10.1016/j.biortech.2013.09.037>.
- Logan, B.E., Hamelers, B., Rozendal, R., Schröder, U., Keller, J., Freguia, S., Aelterman, P., Verstraete, W., Rabaey, K., 2006. Microbial fuel cells: methodology and technology. *Environ. Sci. Technol.* 40, 5181–5192. <https://doi.org/10.1021/ES0605016>.
- Logan, B.E., Call, D., Cheng, S., Hamelers, H.V.M., Sleutels, T.H.J.A., Jeremiasse, A.W., Rozendal, R.A., 2008. Microbial electrolysis cells for high yield hydrogen gas production from organic matter. *Environ. Sci. Technol.* 42, 8630–8640. [https://doi.org/10.1021/ES801553Z/ASSET/IMAGES/ES-2008-01553Z\\_M033.GIF](https://doi.org/10.1021/ES801553Z/ASSET/IMAGES/ES-2008-01553Z_M033.GIF).
- Logan, B.E., Rossi, R., Ragab, A., Saikaly, P.E., 2019. Electroactive microorganisms in bioelectrochemical systems. *Nat. Rev. Microbiol.* 17(5), 307–319. <https://doi.org/10.1038/s41579-019-0173-x>, 2019.
- Love, M.I., Huber, W., Anders, S., 2014. Moderated estimation of fold change and dispersion for RNA-seq data with DESeq2. *Genome Biol.* 15, 1–21. <https://doi.org/10.1186/S13059-014-0550-8/FIGURES/9>.
- Lovley, D.R., Holmes, D.E., 2021. Electromicrobiology: the ecophysiology of phylogenetically diverse electroactive microorganisms. *Nat. Rev. Microbiol.* 20(1), 5–19. <https://doi.org/10.1038/s41579-021-00597-6>, 2021.
- Lustermans, J.J., Sereika, M., Burdorf, L.D., Albertsen, M., Schramm, A., Marshall, I.P., 2024. Extracellular electron transfer genes expressed by candidate flocking bacteria in cable bacteria sediment. *bioRxiv* 2024, 581617. <https://doi.org/10.1101/2024.02.22.581617>, 02.22.
- McMurdie, P.J., Holmes, S., 2013. Phyloseq: an R package for reproducible interactive analysis and graphics of microbiome census data. *PLoS One* 8, e61217. <https://doi.org/10.1371/JOURNAL.PONE.0061217>.
- Mickol, R.L., Eddie, B.J., Malanoski, A.P., Yates, M.D., Tender, L.M., Glaven, S.M., 2021. Metagenomic and metatranscriptomic characterization of a microbial community that catalyzes both energy-generating and energy-storing electrode reactions. *Appl. Environ. Microbiol.* 87. <https://doi.org/10.1128/AEM.01676-21>.
- Mikheenko, A., Prjibelski, A., Saveliev, V., Antipov, D., Gurevich, A., 2018. Versatile genome assembly evaluation with QUAST-LG. *Bioinformatics* 34, i142–i150. <https://doi.org/10.1093/BIOINFORMATICS/BTY266>.
- Minh, B.Q., Schmidt, H.A., Chernomor, O., Schrempf, D., Woodhams, M.D., Von Haeseler, A., Lanfear, R., Teeling, E., 2020. IQ-TREE 2: new models and efficient methods for phylogenetic inference in the genomic era. *Mol. Biol. Evol.* 37, 1530–1534. <https://doi.org/10.1093/MOLBEV/MSAA015>.
- Miyahara, M., Kouzuma, A., Watanabe, K., 2015. Effects of NaCl concentration on anode microbes in microbial fuel cells. *AMB Express* 5, 34. <https://doi.org/10.1186/S13568-015-0123-6>.
- Oksanen, J., Simpson, G., Blanchet, F., Kindt, R., Legendre, P., Minchin, P., O'Hara, R., Solymos, P., Stevens, M., Szoecs, E., Wagner, H., Barbour, M., Bedward, M., Bolker, B., Borcard, D., Carvalho, G., Chirico, M., De Caceres, M., Durand, S., Evangelista, H., FitzJohn, R., Friendly, M., Furneaux, B., Hannigan, G., Hill, M., Lahti, L., McGlenn, D., Ouellette, M., Ribeiro Cunha, E., Smith, T., Stier, A., Ter Braak, C., Weedon, J., 2024. Vegan: community ecology package. R package version, 2.7-0. <https://github.com/vegandevs/vegan>. (Accessed 5 March 2025). <https://vegandevs.github.io/vegan/>.
- Olmsted, C.N., Ort, R., Tran, P.Q., McDaniel, E.A., Roden, E.E., Bond, D.R., He, S., McMahon, K.D., 2023. Environmental predictors of electroactive bacterioplankton in small boreal lakes. *Environ. Microbiol.* 25, 705–720. <https://doi.org/10.1111/1462-2920.16314>.
- Pang, P., Qin, Q., Jiao, Q., He, J., Pang, Z., Wang, L., 2024. New insight into Na<sup>+</sup>-promoted microbial electrolysis cell towards hydrogen energy recovery: feasibility and dual mechanism in salt-containing wastewater treatment. *Chem. Eng. J.* 496, 153623. <https://doi.org/10.1016/j.cej.2024.153623>.
- Paquete, C.M., Morgado, L., Salgueiro, C.A., Louro, R.O., 2022. Molecular mechanisms of microbial extracellular electron transfer: the importance of multiheme cytochromes. *Front. Biosci. - Landmark* 27, 174. <https://doi.org/10.31083/J.FBL2706174/C8AD49D4D863C1DA6639615692D98D1.PDF>.
- Podosokorskaya, O.A., Elcheninov, A.G., Gavrilov, S.N., Petrova, N.F., Klyukina, A.A., Zavarzina, D.G., Merkel, A.Y., 2023. New representatives of the class Ignavibacteria inhabiting subsurface aquifers of yessentuki mineral water deposit. *Water (Switzerland)* 15, 3451. <https://doi.org/10.3390/W15193451/S1>.
- Quast, C., Pruesse, E., Yilmaz, P., Gerken, J., Schweer, T., Yarza, P., Peplies, J., Glöckner, F.O., 2013. The SILVA ribosomal RNA gene database project: improved data processing and web-based tools. *Nucleic Acids Res.* 41, D590. <https://doi.org/10.1093/NAR/GKS1219>.
- Saravanan, A., Kumar, P.S., Duc, P.A., Rangasamy, G., 2023. Strategies for microbial bioremediation of environmental pollutants from industrial wastewater: a sustainable approach. *Chemosphere* 313, 137323. <https://doi.org/10.1016/J.CHEMOSPHERE.2022.137323>.
- Seemann, T., 2014. Prokka: rapid prokaryotic genome annotation. *Bioinformatics* 30, 2068–2069. <https://doi.org/10.1093/BIOINFORMATICS/BTU153>.
- Shi, L., Fredrickson, J.K., Zachara, J.M., 2014. Genomic analyses of bacterial porin-cytochrome gene clusters. *Front. Microbiol.* 5. <https://doi.org/10.3389/FMICB.2014.00657/ABSTRACT>.
- Shi, L., Dong, H., Reguera, G., Beyenal, H., Lu, A., Liu, J., Yu, H.Q., Fredrickson, J.K., 2016. Extracellular electron transfer mechanisms between microorganisms and minerals. *Nat. Rev. Microbiol.* 14, 651–662. <https://doi.org/10.1038/nrmicro.2016.93>, 2016 1410.
- Sun, D., Call, D., Wang, A., Cheng, S., Logan, B.E., 2014. Geobacter sp. SD-1 with enhanced electrochemical activity in high-salt concentration solutions. *Environ. Microbiol. Rep.* 6, 723–729. <https://doi.org/10.1111/1758-2229.12193>.
- Tan, X., Acquah, I., Liu, H., Li, W., Tan, S., 2019. A critical review on saline wastewater treatment by membrane bioreactor (MBR) from a microbial perspective. *Chemosphere* 220, 1150–1162. <https://doi.org/10.1016/J.CHEMOSPHERE.2019.01.027>.
- Tsekouras, G.J., Deligianni, P.M., Kanellos, F.D., Kontargyri, V.T., Kontaxis, P.A., Manousakis, N.M., Elias, C.N., 2022. Microbial fuel cell for wastewater treatment as power plant in smart grids: Utopia or reality? *Front. Energy Res.* 10, 843768. <https://doi.org/10.3389/FENRG.2022.843768/BIBTEX>.
- Velasco, J., Gutiérrez-Cánovas, C., Botella-Cruz, M., Sánchez-Fernández, D., Arribas, P., Carbonell, J.A., Millán, A., Pallarés, S., 2019. Effects of salinity changes on aquatic organisms in a multiple stressor context. *Philos. Trans. R. Soc. B* 374. <https://doi.org/10.1098/RSTB.2018.0011>.
- Wrighton, K.C., Thrash, J.C., Melnyk, R.A., Bigi, J.P., Byrne-Bailey, K.G., Remis, J.P., Schichnes, D., Auer, M., Chang, C.J., Coates, J.D., 2011. Evidence for direct electron transfer by a gram-positive bacterium isolated from a microbial fuel cell. *Appl. Environ. Microbiol.* 77, 7633. <https://doi.org/10.1128/AEM.05365-11>.
- Wu, Y., Zhou, Z., Fu, H., Zhang, P., Zheng, Y., 2022. Metagenomic analysis of microbial community and gene function of anodic biofilm for nonylphenol removal in microbial fuel cells. *J. Clean. Prod.* 374, 133895. <https://doi.org/10.1016/J.JCLEPRO.2022.133895>.
- Xin, X., Xie, J., Li, W., Lv, S., He, J., 2022. New insights into microbial fuel cells for saline wastewater treatment: bioelectrogenesis evaluation, microbial interactions and

- salinity resource reuse. *Process Saf. Environ. Prot.* 168, 314–323. <https://doi.org/10.1016/j.psep.2022.09.077>.
- Yoshizawa, T., Miyahara, M., Kouzuma, A., Watanabe, K., 2014. Conversion of activated-sludge reactors to microbial fuel cells for wastewater treatment coupled to electricity generation. *J. Biosci. Bioeng.* 118, 533–539. <https://doi.org/10.1016/j.jbiosc.2014.04.009>.
- Yu, Y., Lee, C., Kim, J., Hwang, S., 2005. Group-specific primer and probe sets to detect methanogenic communities using quantitative real-time polymerase chain reaction. *Biotechnol. Bioeng.* 89, 670–679. <https://doi.org/10.1002/bit.20347>.
- Zhong, Y., Shi, L., 2018. Genomic analyses of the quinol oxidases and/or quinone reductases involved in bacterial extracellular electron transfer. *Front. Microbiol.* 9, 428022. <https://doi.org/10.3389/fmicb.2018.03029>/BIBTEX.